View Article Online / Journal Homepage / Table of Contents for this issue
Dynamic Article Links

Journal of
Materials Chemistry

Cite this: *J. Mater. Chem.*, 2012, **22**, 8005

www.rsc.org/materials

PAPER

Published on 14 March 2012. Downloaded by National Chiao Tung University on 28/04/2014 23:25:21.

Mechanism of an AZO-coated FTO film in improving the hydrogen plasma durability of transparent conducting oxide thin films for amorphous-silicon based tandem solar cells†

N. Chantarat,[a] Shu-Han Hsu,[b] Chin-Ching Lin,[c] Mei-Ching Chiang[c] and San-Yuan Chen*[a]

Received 5th November 2011, Accepted 23rd February 2012
DOI: 10.1039/c2jm15682b

An Al-doped ZnO (AZO)/F-doped SnO_2 (FTO) film structure in an amorphous silicon solar cell (a-Si:H) was studied under exposure to hydrogen (H) plasma treatment *via* a simple spray pyrolysis. A radio-frequency magnetron sputtering method was used to deposit the FTO film first and the subsequent AZO overlayer on top of the FTO. The results of this approach suggest that the AZO film acts as a protection layer for the underlying FTO film and thus provides an excellent interface that protects the film from the direct bombardment with H^+ ions and radicals. Even under exposure to H-plasma, the optical (UV-Vis) and electrical properties (Hall measurement) of the AZO/FTO double layer film show improvement in plasma stability in comparison with a single FTO film. Without the AZO overlayer, the reduction of SnO_2 to metallic Sn and sub-oxidized SnO can occur in the FTO film. However, after a post-annealing treatment at 400 °C, the degradation of the FTO can be reversed by reoxidizing the Sn–O bonds. This interpretation of the H^+ ion diffusion and the Sn–O redox process is confirmed *via* XPS and SIMS analysis. This investigation provides an opportunity to study the H^+ ion diffusion mechanism in a metal oxide matrix in the presence of plasma and thermal effects. The study thus provides an alternative to the conventionally used FTO-based Si solar cells.

Introduction

Hydrogenated amorphous silicon (a-Si:H) solar cells have generated intense interest as an alternative to crystalline silicon cells because of the low cost preparation procedure. These cells provide the functions of light absorption and charge carrier transport that takes place at the transition of a multijunction p–i–n diode[1,2] (interface region), sandwiched between the transparent conductive oxide (TCO) layer and the back contact layer. In general, amorphous silicon thin films are grown using plasma-enhanced chemical vapor deposition (PECVD) by exposing the sample to silane plasma, which contains hydrogen radicals and ions. Therefore, one of the key problems is the enhanced reduction of tin oxide in the TCO layer, caused by the generation of hydrogen (H) atoms on interstitial (H_i) and substitutional (H_O) defect sites. Once a certain incorporation of defects is achieved, a significant degradation in the electrical, optical and even structural properties has been observed in a number of studies.[3–5]

In addition, another class of transparent-conducting materials that includes Al-doped ZnO (AZO) has received significant attention not only for its excellent electronic and optical properties, comparable with F-doped SnO_2 (FTO) or Sn-doped In_2O_3 (ITO), but also for its high durability under exposure to thermal annealing and H-plasma treatment.[6–10] However, AZO films produced by sputter deposition tend to display a flattened surface, which causes lower haze values. Therefore, from an architectural point of view, textured FTO films are generally fabricated by high temperature deposition using various methods in which a controllable film growth morphology is employed to enhance the light scattering and haze ratio for the TCO electrode.[11–13]

A number of fabrication strategies have been successfully utilized to generate a double-layer TCO electrode.[14,15] However, these reports have mainly examined the effects of the successive preservation of the FTO film by an alternative protection layer. For example, the application of an a-Si_3N_4:H barrier layer on top of the SnO_2 layers was proposed to reduce the diffusion of decomposed Sn atoms into the p-type a-$Si_{1-x}C_x$:H ($x = 0.28$), and X-ray photoelectron spectroscopy (XPS) revealed the formation of chemical bonds between the Sn and other elements, such as Si, C and N, according to the diffusion mechanism of Sn.[1] Recently, to overcome disadvantages, such as low conductivity,

[a]Department of Materials Science and Engineering, National Chiao Tung University, 1001 Ta-Hsueh Road, Hsinchu, Taiwan, Republic of China. E-mail: sanyuanchen@mail.nctu.edu.tw; Fax: +886-3-5725490; Tel: +886-3-5731818
[b]National Nano Device Laboratories, No. 26, Prosperity Road I, Science-Based Industrial Park, Hsinchu, Taiwan, Republic of China
[c]Materials and Chemical Research Laboratories, Industrial Technology Research Institute, Chutung, Hsinchu, Taiwan, Republic of China
† Electronic supplementary information (ESI) available. See DOI: 10.1039/c2jm15682b

Published on 14 March 2012. Downloaded by National Chiao Tung University on 28/04/2014 23:25:21.

low transparency and poor durability of the coated films, a double-layer TCO film composed of binary compound oxides (In-doped ZnO/F-doped SnO_2) has been utilized as a transparent electrode for a-Si:H solar cells.[8] Unfortunately, the production of In-doped ZnO films requires high temperatures (>375 °C) in order to deposit a rough and thick layer on the FTO glass, which degrades the original FTO properties. Accordingly, the interfacial effect of the epitaxially grown films is another important factor that controls the atomic diffusion behavior. Attempts to examine further the properties of this structure under H-plasma treatment and to understand the effects of thermal annealing have not yet been undertaken.

Therefore, we propose a double-layer TCO electrode that involves an additional barrier layer of AZO above the FTO layer. In this configuration, the original morphology of the FTO remains, while the deterioration of the FTO film properties can be reduced, even in the presence of a plasma atmosphere containing hydrogen radicals and ions. Moreover, we also investigated the diffusion of incorporated hydrogen in the double layer AZO/FTO films *via* a change in the chemical composition and a reversal of the deterioration. This effect was achieved by performing a post-annealing treatment (at a higher temperature than that observed during the plasma treatment) following the plasma process. A comparison between the results of the as-deposited, plasma treated and post-annealed samples for a variety of single and double layer films provides an improved understanding of the surface and bulk characterization, as determined by the analysis of the structural, electrical and optical properties. Presumably, the investigation of these reproducible double TCO films could lead to a significant development in the generation of efficient a-Si:H solar cell devices.

Experimental

An FTO solution was prepared *via* a chemical route for the sake of high solubility. The precursor solution containing a mixture of $SnCl \cdot 4H_2O$ (1 mM) and NH_4F (0.5 mM) was dissolved in 500 ml of DI water. To improve the solubility of the solution, 10 ml of HCl was added into the solution and stirred vigorously (~30 min) until the solution turned transparent.[15–17] The resulting solution was placed in an ultrasonic nebulizer reactor, which produced an aerosol with a controlled droplet size distribution in the range of 1–3 μm and an output deposition speed of 3 ml min^{-1}. The precursor was pyrolyzed on the heated substrate. The substrate holder was equipped with thermocouples and heating elements, which were managed by a temperature controller. The deposition process was carried out under atmospheric conditions for 5 min on a heated Corning glass substrate at 420 °C, where a film growth rate of approximately 50 nm min^{-1} could be expected. Subsequently, the AZO film was deposited on the top side of the FTO film by a radio frequency magnetron sputtering system, using a commercial AZO target. The substrate temperature was kept below 80 °C, and the sputtering power was 100 W. The base pressure of the system and the pressure during sputtering of 1.5×10^{-2} mTorr were controlled by a combined vacuum system of mechanical and turbomolecular pumps supplying high-purity Ar gas into the main chamber. The annealing process took place at 300 °C. The sample preparation produced an AZO film with constant thickness that depended on the deposition duration (15 min).

For this investigation, all films were prepared using different geometries for comparison: individually deposited single layers of FTO and AZO and a double layer consisting of AZO and FTO films were then exposed to hydrogen plasma. The hydrogen plasma was generated by high density plasma chemical vapor deposition (HDP-CVD, Duratek systems) from H_2 gas with a flow of 20 sccm and a pressure of 100 mTorr. The inductively coupled plasma (ICP) in the HDP-CVD was a high-density mixture of gases at low pressure. The bias voltage was held constant at 10 V, and the RF power was 200 W. The samples were examined to quantify the hydrogen radical durability of the films by varying the plasma duration from 0 to 5, 10, 20 and 30 min at a substrate temperature of 250 °C. In addition, to investigating the recovery of the deteriorated film properties, the plasma treated samples were post-annealed at 400 °C.

The analysis of the film morphology and thickness was performed using a scanning electron microscope (JEOL JSM-6700F) and a high resolution transmission electron microscope (JEOL 2100). A focused ion beam system (FEI, Nova NanoLab 600) was used to prepare the cross-sectional sample for TEM imaging. Focused ions at a 30 keV acceleration potential and a 5 pA beam current were used to sputter away atoms from the surface. This technique allows material dependent selective etching to create a specific interest area for cross-sectional TEM observation. The crystalline structure of the films was characterized using an X-ray diffractometer (XRD) equipped with a Cu-Kα radiation source. UV-Vis spectroscopy was employed to determine the effect of hydrogen incorporation on the optical transmission spectra of the deposited films in the wavelength range of 300–700 nm. To determine the electrical properties, Hall effect measurements were carried out at room temperature using a Van der Pauw sample configuration (with a magnetic field of 4000 Gauss and an electric current of 0.1 mA) with indium balls as the Ohmic electrode. Secondary ion mass spectroscopy (SIMS) measurements were performed by the CAMECA IMS 7f, which is a double-focusing magnetic sector SIMS with a 15 keV Cs^+ primary excitation beam. The SIMS depth profiles revealed the diffusion behavior of hydrogen ions into the films. All such quantitative analyses were measured alongside a homogeneous reference standard composed of the same mineral or material, in order to correct for variations in ion yields that depend both on the chemistry and structure of the matrix.

The XPS spectra were obtained on a Physical Electronics Quantera Scanning X-ray Multiprobe instrument, which was equipped with a monochromatic Al Kα X-ray source operated at 1486.6 eV and 26.18 W. The spectra were referenced to the main C1s peak at 284.0 eV. The X-ray beam size was 100 μm, and the data were collected from surface areas of 100 μm × 300 μm with a pass energy of 224 eV and a step energy of 0.4 eV for high resolution scans. The measurements were collected after 25 scanning cycles.

Results and discussion

Fig. 1 shows SEM images of a single layer FTO film and a double layer AZO-coated FTO film under H-plasma treatments of various durations (0–30 min). As shown in Fig. 1(a–c), the FTO

This journal is © The Royal Society of Chemistry 2012

View Article Online

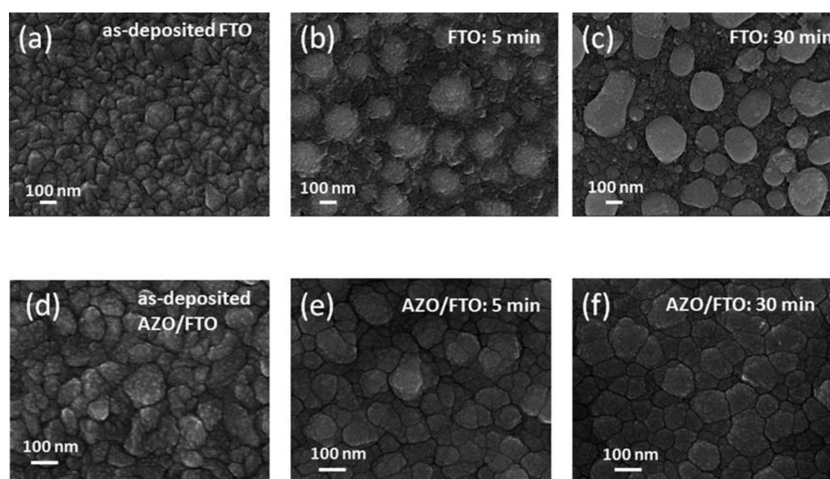

Fig. 1 Plane-view SEM images of the textured FTO films and the AZO/FTO films (a and d) without H_2 plasma treatment or with H_2 plasma treatment for (b and e) 5 min, and (c and f) 30 min.

Published on 14 March 2012. Downloaded by National Chiao Tung University on 28/04/2014 23:25:21.

film has a grain size in the range of 50–150 nm. After H-plasma treatment for 5 min, the surface morphology began to produce small white particles because of the disintegration of the original FTO grains. As the H treatment time increased to 30 min, the white area became more apparent, and larger stacks (approximately 300 nm in grain size) were formed. These stacks are assumed to be integrated from ultrafine Sn nanoparticles moving up from the surface of the film. In Fig. 1(d–f), the morphology of the deposited AZO layers has a granular surface coverage on top of the FTO surface. The size of the fine AZO particles formed on the crystalline FTO surface by secondary nucleation was measured to be approximately 10–20 nm. As the plasma treatment duration increased, the AZO/FTO was able to retain its original morphology because of the protection from a barrier AZO layer. The corresponding cross-section SEM images of the AZO, FTO and double AZO/FTO films are also shown in Fig. S1.†

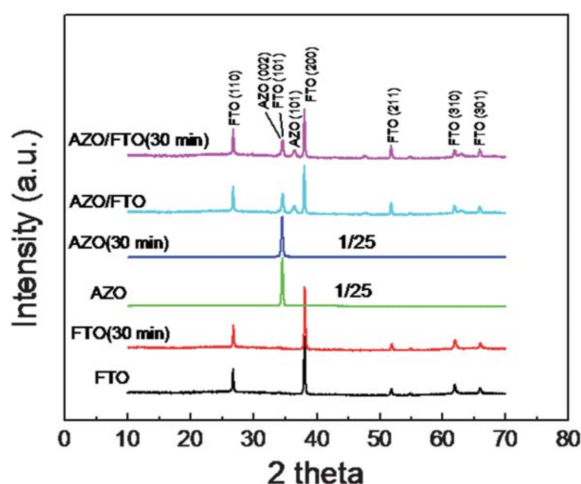

Fig. 2 X-ray diffraction patterns of the FTO, AZO, and AZO/FTO samples before and after H_2 plasma treatment for 30 min, as identified on each spectrum.

Fig. 2 shows the XRD patterns for the FTO, AZO and AZO/FTO films before and after the plasma process. The diffractogram of the FTO film shows the existence of the (110), (101), (200), (211), (310) and (301) peaks, which correspond primarily to SnO_2 polycrystalline planes, whereas the AZO film has a single peak dominated by the (002) orientation of crystalline ZnO. Moreover, the combined AZO/FTO double layer film also shows crystallites of the two metal oxide compounds. Following the post H-plasma heat treatment at 250 °C, there are no additional diffraction peaks that belong to other non-relative compositions in the treated films compared with the as-deposited films; this result indicates that H^+ ion bombardment and thermal effects do not distort the crystallinity of the lattice structure. The full width at half maximum (FWHM) of the main FTO, AZO and AZO/FTO peaks were approximately calculated as the ratios between their values before and after the 30 min H-plasma treatment (1 : 1, 1 : 0.9 and 1 : 1, respectively), which indicates an unchanged crystallite size. The XRD results are also consistent with the cross-sectional TEM analysis of the AZO/FTO samples under plasma treatment, as shown in Fig. 3(a).This result reveals that the FTO film exhibits the columnar growth of pyramidal shapes with a thickness of approximately 240 nm, which are covered by an AZO layer of approximately 70–90 nm in thickness. Compared to bare FTO and AZO films on the Si substrate (Fig. S2†), no apparent difference can be identified. The AZO/FTO sample was also coated with Pt to facilitate the preparation of the cross-sectional TEM samples using the focused ion beam (FIB) method.

A thin continuous AZO layer was formed as a result of the low surface energy of the FTO, and it could completely bridge the gap at the interface. Both the FTO and AZO layers exhibited clear lattice fringes that separated one another from the atomically sharp interface. Therefore, although the samples were exposed to plasma for 30 min, Fig. 3(b) clearly demonstrates that the lattice fringes of the individual pyramids in each FTO grain could remain crystallographically aligned along the same direction [200] with respect to the preferential orientation. The spacing between two adjacent lattice planes remains constant at

Published on 14 March 2012. Downloaded by National Chiao Tung University on 28/04/2014 23:25:21.

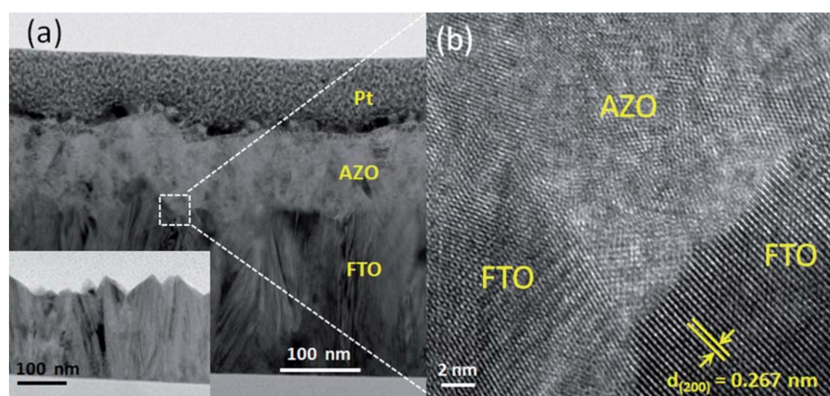

Fig. 3 (a) Cross-sectional TEM image of an AZO/FTO film coated by a thin Pt conductive layer. The inset shows a single FTO film deposited on a bare glass substrate. (b) High-magnification TEM image taken from the region, marked by a square in (a).

approximately 0.267 nm, which is consistent with the (100) plane of SnO_2 in the rutile structure.

The dependence of the Hall measurements (the carrier concentration (n), the Hall mobility (μ) and the sheet resistance (R_s)) on the length of the H-plasma treatment is illustrated in Fig. 4(a), 4(b) and 4(c), respectively. For the FTO samples, the carrier concentration decreased from a maximum of 6.61×10^{20} to 5.36×10^{20} cm^{-3} after 30 min. In other words, the mobility gradually increased from 12.83 to 16.52 cm^2 V^{-1} s^{-1} after a plasma treatment of up to 20 min. This trend is inversely proportional to the lower carrier concentration as a consequence of the decrease in the number of electron scattering centers.[7] However, the mobility decreased significantly to 12.35 cm^2 V^{-1} s^{-1} when the treatment time was increased to 30 min. This result indicates that surface scattering may occur from the grain boundary effect because a large number of H radicals are likely to be dispersed at the grain boundaries or around the FTO particles.[6,8] Thus, the formation of accumulated stacks on the surface, as shown in the earlier SEM image (Fig. 1(c)), can hinder the charge transport across the boundaries. In principle, this effect implies that the characteristics of the mean free path of the carriers must be changed by an increase in the potential-well barrier at the depleted region. Fig. 4(c) shows that the sheet resistance of the samples increases upon hydrogen radical treatment, which could be attributed to the change in the composition of the surface layer from SnO_2 to SnO or SnO_{1-x}. This result is consistent with the report by Wallinga *et al.*[3] It is implied that the reduction of the ambient hydrogen during hydrogen plasma treatment can cause a greater loss of oxygen and a decrease in the conductivity of the FTO films because of the reduction of the properties of the tin oxide. This result expresses and demonstrates the formation of intrinsic defects (V_O) in the film. Thus, it is also in good agreement with the 2-fold increase in sheet resistance observed after the plasma treatment.[10]

However, both the carrier concentration and the mobility of the AZO film increase with increasing plasma duration, although they remain constant after a certain amount of treatment time because of the saturation of H absorption. Interestingly, a dramatic reduction in the sheet resistance was observed after 5 min (from 16.78 to 11.05 Ω □$^{-1}$), which was dependent on the variation in the carrier concentration, as shown in Fig. 4(a). Indeed, this result indicates that the plasma-enhanced conductivity is a result of surface-related electron transport, rather than a bulk effect. Hydrogen plasma allows the chemisorption of H impurities on the surface; therefore, interstitial H atoms with small migration energies can subsequently form hydroxyl (OH) groups with their nearest-neighbor O atoms, which act as shallow donors in the ZnO.[6,7,9] The XPS measurements have been performed as shown in Fig. S3 in the supporting information.† The O 1s level peak in the spectrum of SnO_2 was fitted by two Gaussian functions, which were centered at 530.7 eV and 531.8 eV. The low binding energy component is attributed to the crystal lattice oxygen in rutile tin dioxide in agreement with the reported binding energy, BE = 530.6 eV. The high binding energy broad component is assigned to the O_2^-or OH^- surface groups of the tin oxides.[18] In our case, the as-deposited FTO film shows a strong low-binding-energy component, but the high-binding-energy component was enhanced after H-plasma

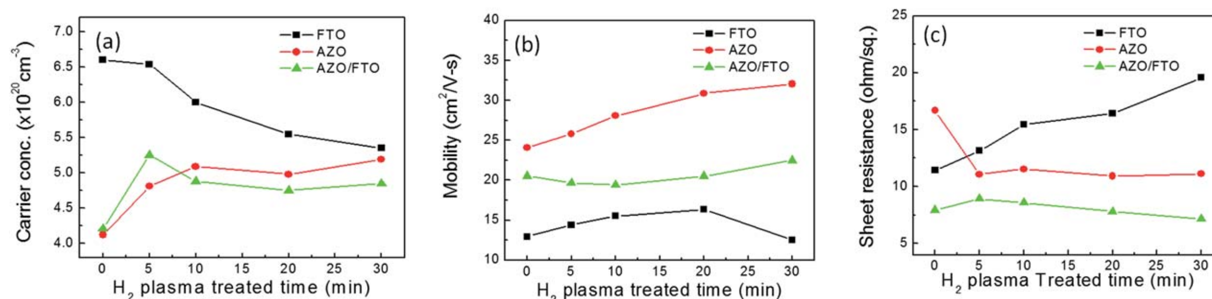

Fig. 4 Dependence of (a) carrier concentration, (b) Hall mobility, and (c) sheet resistance on the H_2 plasma treated time for the deposited FTO, AZO, and AZO/FTO films.

 This journal is © The Royal Society of Chemistry 2012

View Article Online

Published on 14 March 2012. Downloaded by National Chiao Tung University on 28/04/2014 23:25:21.

treatment, which indicates the formation of OH and a variation in the concentration of OH groups. The trend of the Hall effect (n, μ and R_s) variations in our results shows relatively good agreement with the literature, as shown in refs. 6, 7, 9. However, after longer plasma treatment, the H atoms are expected to diffuse towards deeper levels through a hopping process, which is associated with the rebinding of the second-neighbor O atom.[10] Indeed, the donor concentration, as well as the generation of free electrons, becomes enhanced, thereby leading to improved conductivity of the H-incorporated AZO film relative to the untreated one.

In the double layer AZO/FTO film, the mobility varied slightly as a function of the plasma treatment time, while the other electrical characteristics (n and R_s) improved after a 5 min treatment. The results can be explained in the following manner. (1) The Hall effect is considered to be a surface-related measurement; consequently, the enhanced electrical properties of the entire AZO/FTO film are mainly caused by the high conductivity of the AZO film layer. (2) When the H-plasma treatment exceeded a given amount of time (10–30 min), it may induce the further diffusion of hydrogen toward a deeper level and its accumulation at the interfacial layer between the AZO and FTO films, as confirmed by the SIMS analysis. In these conditions, the partial H^+ ions presumably disintegrate the SnO_2 of the uppermost crystalline FTO film, causing the surface desorption of metallic Sn[3,4] and the property degradation of the FTO film. Subsequently, the depletion of an ultrafine thin layer occurs from the migration of structural defects (misfit dislocations) to the regions of lower diffusion coefficient at the bottom of the AZO layer.[2] Nevertheless, examination of the AZO layer has proven that the H atoms are mostly prevented from annihilating a portion of the FTO layer, which can preserve the contact properties by limiting metallic interdiffusion and the accumulation of impurities. On the basis of the above statements, it is implied that the slight variation in properties could be attributed to the compromise between phenomena (1) and (2) in the equilibrium state.

In the presence of H-plasma, the FTO samples in Fig. 5(a) exhibit a change in their UV-Vis spectra, wherein the optical transmission gradually diminished from 99.6 to 31.6% at a wavelength of 550 nm as the duration of the plasma treatment increased from 0 to 30 min. The combination of the structural and optical data shows that the FTO films were deteriorated by H-incorporated radicals because of the reduction of SnO_2 to metallic Sn and the sub-oxide of Sn (SnO). Because both excess Sn and SnO may create crystal disorder and trap electron carriers, the reduction of the optical band gap is expected as the valence band (VB) moves up and the conduction band (CB) moves down. The dominant intrinsic defects (Sn_i and V_O) in SnO_2 are compensated for by the presence of metallic Sn and SnO, which lower the carrier density and cause a decrease in the refractive index (n).[11] Moreover, the absorption edge shifts towards a longer wavelength (lower energy) for all the H-treated samples in Fig. 5(a); this effect is ascribed to the decreased carrier concentration caused by surface roughness, as presented in Fig. 4(a). According to the above reasons, the formation of the SnO texture has a remarkable effect, inducing greater light scattering and optical trapping in the film.

However, the transmittance of the deposited AZO/FTO samples in Fig. 5(b) did not show any dependence on the H^+ ion energy with increasing exposure times. All of the samples show average transmission values of more than 80% in the spectral range of 400–700 nm, although a slight shift in the absorption peaks is observed because of the addition of H-related point defects, such as Zn interstitials (Zn_i) and oxygen vacancies (V_O). Theoretically, this effect occurs because the H-incorporated atoms containing H_i and H_O are coordinated at interstitial (lying in a Zn–O bond-centered position) and substitutional O sites, respectively. Only H_i with its high mobility and low formation energy, rather than H_O, can easily migrate from its original position to its preferential position, and H_i is likely to form a O–H bond with the nearest-neighbor O atoms. Therefore, there will not be substitution of H atoms at the O sites (H_O) in ZnO, leading to the dissociation or reformation of Zn–O bonds, unless the formation energy is high enough to overcome the oxygen chemical potential (μ_O).

To examine whether the heat treatment could indeed cause recovery of the optoelectronic properties of plasma-treated films, all samples were subsequently placed in an oven at 400 °C for 1 h. During the thermal treatment, the heat flow was expected to be isotropic and to expel the diffusion of H atoms either upward or downward in the film interlayer, which is suitable to provide an understanding of the reversible thermal mechanism. Fig. 5(c) and 5(d) show the optical transmission after the post-annealing process for the FTO and AZO/FTO films, respectively. Clearly, there is an increase in the transmission in Fig. 5(c) back to the original value (that of as-deposited FTO). As a result, the 5 and 10 min plasma treated samples show nearly a complete recovery, which is not the case for the samples treated for 20 and 30 min. Although any particular H_O is stable enough to occupy an O site, the annealing treatment at 400 °C is high enough to break a multicenter bond of Sn–H to release the unbound Sn. The thermal treatment suggests that at short H-plasma treatment durations (5 and 10 min), the H^+ ions are able to escape from the film, while the Sn is reoxidized to form the SnO_2 phase as a result of the appropriate annealing conditions. However, longer treatment times (20 and 30 min) might affect other physical properties by permanently changing the surface morphology of the FTO films. In that case, the severely damaged film containing a large amount of suboxide SnO did not result in the recovery of optical transmission. When pure FTO was compared with the double AZO/FTO films, it was found that fringes were present at short wavelengths of the UV-Vis spectra, which is related to the fact that FTO has a larger band gap (4.4 eV) than AZO (3.2 eV) and has good transmission properties at short wavelengths. Therefore, the AZO/FTO double layer structure displays different optical transmission characteristics from those of the FTO film because of the absorption at short wavelengths by the AZO material, which causes the presence of fringes in the spectra and their variation.

Fig. 6 displays the concentration profiles of Sn, O, F and H as a function of the depth determined by SIMS for both a single layer of FTO and a double-layered AZO/FTO film deposited on a Corning glass substrate. The intensity shows the variation in concentration with respect to the Cs^+ ion etching depth (nm) for the plasma-treated samples (S2) and the post-annealed samples at 400 °C (S3). One region in the single FTO film (225 nm) is clearly identified in Fig. 6(a–b), while the AZO-coated FTO film contains two main regions (440 nm) with a constituent interfacial

View Article Online

Published on 14 March 2012. Downloaded by National Chiao Tung University on 28/04/2014 23:25:21.

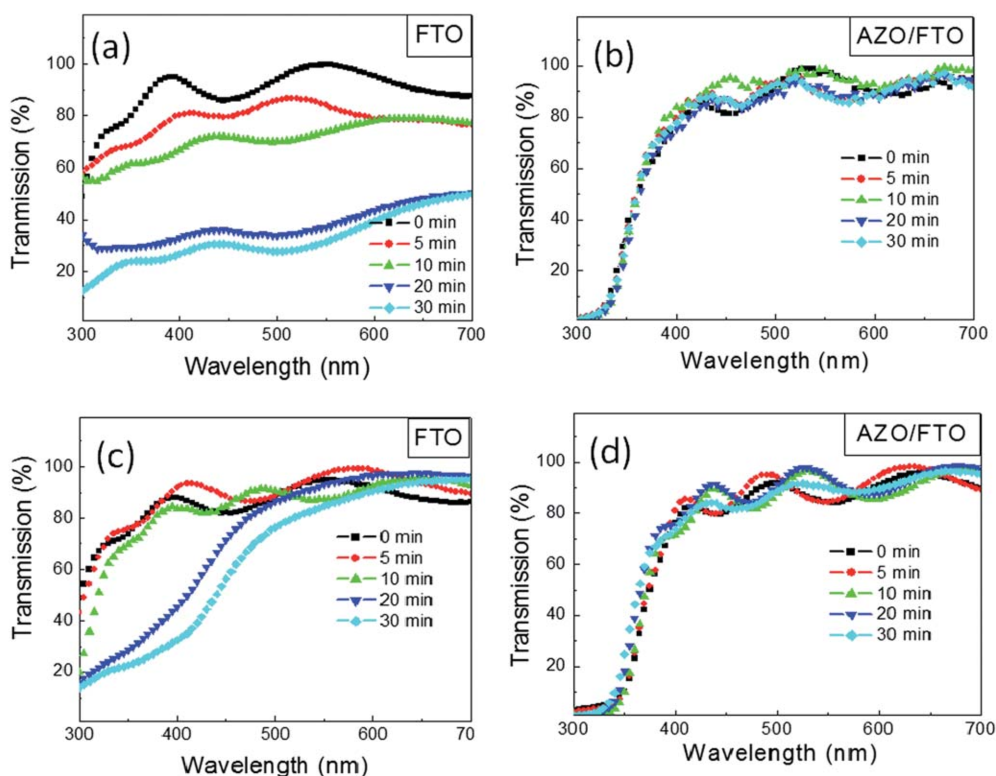

Fig. 5 The effect of (a and b) H_2 plasma treatment at 0, 5, 10, 20 and 30 min, and (c and d) post-annealing treatment at 400 °C on the optical transmission of the FTO and AZO/FTO films.

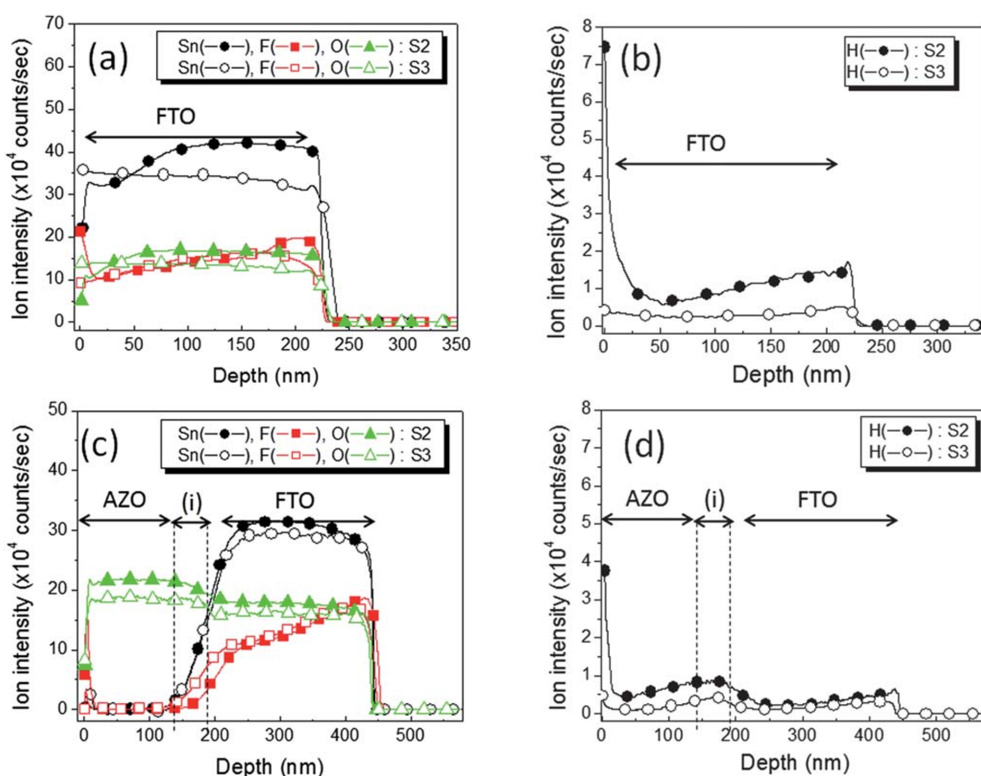

Fig. 6 SIMS depth profiles of (a and b) FTO and (c and d) AZO/FTO films for the secondary ion count of Sn, F, O, and H normalized relative to FTO. The plasma-treated samples and the post-annealed samples are represented by S2 and S3, respectively.

This journal is © The Royal Society of Chemistry 2012

View Article Online

Published on 14 March 2012. Downloaded by National Chiao Tung University on 28/04/2014 23:25:21.

region, as shown in Fig. 6(c–d). First of all, it should be noted that neither the Zn nor Al signals were visible in this profile because only H-affected elements with high intensity were assigned to interpret the relative changes in their chemical compositions. In Fig. 6(a), the severe damage caused by H^+ ion incorporation (S2) may have caused the reduced intensity of the Sn and O signals in the near-surface region (<75 nm in depth), compared to their intensity in the in-depth region, because of the presence of metallic Sn or SnO, which mainly causes the surface roughness mentioned earlier. After the annealing process (S3), the Sn and O signal intensities change significantly to nearly a constant value, demonstrating the reoxidization and recovery of the film. Meanwhile, the amounts of both H and F ions were noticeably reduced because of the thermally-enhanced diffusion, especially at the surface and the bottom of the film. In addition, the XPS spectra in the supporting information (Fig. S4†) provide further insight into the effect of H incorporation for the FTO film, derived from the binding energy of the $Sn3d_{3/2}$ and $Sn3d_{5/2}$ electrons, a common signature of the Sn oxidation states (Sn^{4+}), corresponding to the equilibrium O–Sn–O species bound to the SnO_2 framework. These results indicate that the plasma (S1 to S2) and post annealing (S2 to S3) treatments of the FTO samples introduce decomposition and reoxidization of the Sn–O bonds, respectively.

In Fig. 6(c), a clear separation between the AZO and FTO layers is identified as the interfacial region "(i)", where the Sn and F signal intensities increase drastically, indicating the beginning of the main components of the FTO films and the appearance of their maximum intensities at the stoichiometric point corresponding to the O signal intensity. Similar to the single FTO film in Fig. 6(b), Fig. 6(d) shows the accumulation of H^+ ions at the surface and in the interfacial region, where it is assumed to have a lower surface energy compared with the mid-layer regions.[19] After the subsequent annealing process (S3), only slight changes in the Sn and O intensities were observed. Because the AZO coated layer prevented the dissociation of the FTO film from H^+ ion incorporation, the variation of the intensities of all matrix elements showed only small changes between S1–S2 (decomposition) and S2–S3 (reoxidization or recovery).

To probe the detailed electronic structure of the FTO and AZO/FTO films, we used XPS to investigate the oxidation states at the surface. In our case, clear fluorine peaks were detected in both film types. The chemical bonding compositions of the F dopant and the Sn element were examined by following a sequential process. The as-deposited, H-plasma and post-annealing films were defined as S1, S2 and S3, respectively. For S1, the primary spectra in Fig. 7(a) and 7(b) do not show any F 1s peaks because of the very low F doping concentration in the SnO_2. Therefore, no signals corresponding to fluorine or its ionic form can be detected at this stage. Interestingly, after undergoing the H-plasma process (S2) for 30 min, the binding energy (BE) of the F 1s peak for the single-layer FTO, and the double-layer AZO/FTO films appears at 684.8 eV. This peak is composed of two deconvoluted peaks at 684.7 and 687.5 eV, which are assigned to F_1 and F_2, respectively. Suffner *et al.* reported that the replacement of oxygen with fluorine can form Sn–F and C–F groups incorporated into the FTO films.[13] Furthermore, it has been proven by the calculation of the structure factors that fluorine atoms prefer to occupy substitutional oxygen sites at a low doping level, rather than being incorporated as interstitials.[20] As a result, it can be assumed that the replacement of oxygen with fluorine may have changed the doping behavior because of the incorporation of H atoms. This effect occurs because the interstitial hydrogen has a low formation energy and a high mobility to react with the ion-absorbed oxygen (O^{2-}) in SnO_2 to form strong O–H bonds. In addition, the reaction between the H and O atoms could potentially have a great impact on the release of the F dopant from the O sites and the reduction of the SnO_2 to a suboxide (SnO_x) or metallic tin (Sn), leading to the loss of electrical conductivity. Because fluorine (F_i) is known to be one of the most reactive and electronegative elements, a consequential ionic fluoride bond, such as a Sn–F, could be readily formed on the surface of the film. Thus, the deconvoluted F_1 peak at low binding energy is the major component, representing the Sn–F bond complex. In other words, an F_2 shoulder can be observed in the F 1s peak located at high binding energy, where the negligible peak is assigned to the C–F bonds that probably arise from the carbonaceous species in the atmosphere[12] and are often found in the powder form. The intensity of F_2 is much lower than that of ionic fluoride (F_1) because the carbon–fluorine bond is much weaker and less dense in the FTO film;[13] consequently, it is susceptible to thermally induced desorption from the crystalline solid surface.

Furthermore, we note that the single-layer FTO sample is much more disrupted than the double-layer AZO/FTO film in the presence of increasing H content above a critical value because the major F_1 peak of the FTO film shows an increase in the formation of Sn–F bonds, while the AZO/FTO film shows a 2-fold decrease at the same intensity. The difference between the peak intensities of the two films suggests that the barrier AZO layer partially prevented severe damage caused by H-ion bombardment from occurring on the FTO film. At the final stage (S3), the samples were annealed at 400 °C for 1 h to examine the desorption behavior of the H atoms. For the FTO sample, the peak nearly disappeared because of thermal perturbation, which takes place in the presence of reoxidized SnO_2. In contrast, a small amount of the F_1 peak in the AZO/FTO sample could be observed, which may represent the residual Sn–F bonds located in the interfacial layer between the AZO and FTO films, particularly at grain boundaries.

Overall, a reversible mechanism for H diffusion within the FTO and AZO/FTO films can be explained in Scheme 1 in the following manner. (1) For FTO films, during the H-plasma treatment, H^+ accumulated in the FTO film at a certain depth, but later annealing treatment promoted H-atom migration and released H-atoms outward to the surface from their accumulation in the FTO layer. Consequently, the film properties made a partial recovery to those of the as-deposited film, unless the film surface was permanently damaged by extended plasma treatment (20–30 min). (2) For the AZO/FTO film, the AZO-coated layer acted as the barrier layer to block certain H^+ ions from diffusing into the underlying FTO layer. In these conditions, the H atoms were mostly distributed in the AZO layer, which strongly reduced the FTO and dissociated the Sn–O bonds at the interface between the AZO and FTO layers. Therefore, the H-atoms tended to accumulate at the AZO/FTO interface and at the surface of the FTO layer, as indicated by the SIMS depth profile of H in Fig. 6(d), but when the sample underwent the

View Article Online

Published on 14 March 2012. Downloaded by National Chiao Tung University on 28/04/2014 23:25:21.

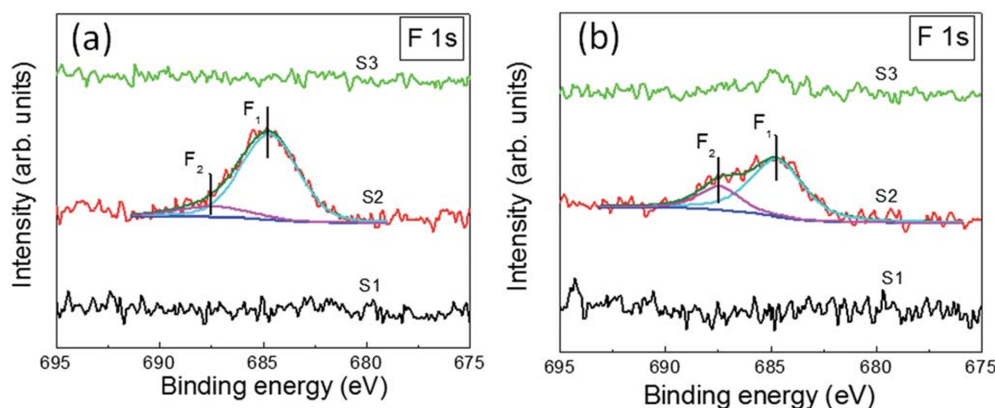

Fig. 7 X-Ray photoelectron spectra of the F 1s peak observed for (a) FTO and (b) AZO/FTO samples with as-deposited conditions (S1), 30 min plasma treatment (S2), and a post-annealing process, subsequently. The deconvoluted peaks F_1 and F_2 indicate a major component (Sn–F bond) and a minor component (C–F bond), respectively.

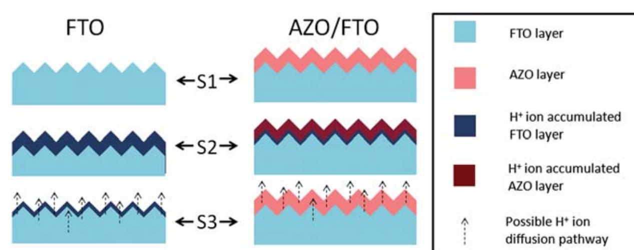

Scheme 1 Illustration showing the cross-sectional structure of FTO and AZO/FTO films and the possible H^+ ion diffusion mechanism under different conditions.

post-heating process, the H-treated AZO layer showed identical H diffusion behavior to that of the single FTO film.

Conclusion

In summary, two types of films—a single-layer FTO film and a double-layer AZO/FTO film—were investigated for use as the transparent conducting oxide layer in hydrogenated amorphous silicon (a-Si:H) solar cells. Compared to AZO films, FTO films are easily grown with a columnar structure, and they display a rough surface morphology, which is beneficial for their optical transmission for solar-cell light absorption to enhance the power conversion efficiency. However, in the presence of a plasma atmosphere containing hydrogen radicals and ions, the results show that the surface of the bare FTO films can deteriorate because of the reduction of SnO_2 to metallic Sn and the SnO sub-oxide by H^+-incorporated ions and radicals encountered in the H-plasma treatment. In contrast, the AZO overlayer was found to conserve the structural, electrical, and optical properties of the FTO film. Furthermore, the post-heat treatment (400 °C) caused the recovery of the degraded FTO films. Thus, combining the individual advantages of FTO and AZO into double TCO films (AZO/FTO) provides a significant development for the generation of efficient FTO-based Si solar cell devices. This strategy was proven to be convenient and effective for a-Si:H solar cells, while the incorporation and diffusion of H^+ ions into the matrix is necessary for the development of multilayer films with designed interfaces and improved properties.

Acknowledgements

This work was financially supported by the National Science Council of the Republic of China, Taiwan under Contract NSC100-3113-E-009-002. We also thank the Industrial Technology Research Institute of Taiwan for technical and financial support.

References

1 H. Stibig, F. Siebke, W. Beyer, C. Beneking, B. Rech and H. Wagner, *Sol. Energy Mater. Sol. Cells*, 1997, **48**, 351–363.
2 T. Hayashi, K. Kawabata, K. Yamada, S. Miyazaki and M. Hirose, *Jpn. J. Appl. Phys.*, 1991, **30**, 675–678.
3 J. Wallinga, W. M. Arnoldbik, A. M. Vredenberg, R. E. I. Schropp and W. F. Van der Weg, *J. Phys. Chem. B*, 1998, **102**, 6219–6224.
4 S. Major, M. C. Bhatnagar, S. Kumar and K. L. Chopra, *J. Vac. Sci. Technol., A*, 1988, **6**, 2415–2420.
5 K. Xiong, J. Robertson and S. J. Clark, *J. Appl. Phys.*, 2007, **102**, 083710.
6 K. Ahn, Y. S. Jeong, H. U. Lee, S. Y. Jeong, H. S. Ahn, H. S. Kim, S. G. Yoon and C. R. Cho, *Thin Solid Films*, 2010, **518**, 4066–4070.
7 S. H. Lee, T. S. Lee, K. S. Lee, B. Cheong, Y. D. Kim and W. M. Kim, *J. Phys. D: Appl. Phys.*, 2008, **41**, 095303.
8 C. H. Lee, K. S. Lim and J. Song, *Jpn. J. Appl. Phys.*, 1997, **36**, 4418–4422.
9 C. Van de Walle, *Phys. Rev. Lett.*, 2000, **85**, 1012–1015.
10 J. Bang and K. J. Chang, *Appl. Phys. Lett.*, 2008, **92**, 132109.
11 H. Kim, C. M. Gilmore, A. Piqué, J. S. Horwitz, H. Mattoussi, H. Murata, Z. H. Kafafi and D. B. Chrisey, *J. Appl. Phys.*, 1999, **86**, 6451–6461.
12 A. I. Martínez, L. Huerta, J. M. O. Rueda de León, D. Acosta, O. Malik and M. Aguilar, *J. Phys. D: Appl. Phys.*, 2006, **39**, 5091–5096.
13 J. Suffner, P. Ágoston, J. Kling and H. Hahn, *J. Nanopart. Res.*, 2010, **12**, 2579–2588.
14 J. H. Noh, S. Lee, J. Y. Kim, J. K. Lee, H. S. Han, C. M. Cho, I. S. Cho, H. S. Jung and K. S. Hong, *J. Phys. Chem. C*, 2009, **113**, 1083–1087.
15 T. Kawashima, T. Ezure, K. Okada, H. Matsui, K. Goto and Tanabe, *J. Photochem. Photobiol., A*, 2004, **164**, 199–202.
16 N. Chantarat, Y. W. Chen, C. C. Lin, M. C. Chiang and S. Y. Chen, *Inorg. Chem.*, 2010, **49**, 11077–11083.
17 C. C. Lin, Y. W. Chen, M. C. Chiang, C. H. Lee, Y. L. Tung and S. Y. Chen, *J. Electrochem. Soc.*, 2010, **157**, H227–H230.
18 T. Kawabe, S. Shimomura, T. Karasuda, K. Tabata, K. Suzuki and Y. Yamaguchi, *Surf. Sci.*, 2000, **448**, 101–107.
19 J. C. Liu, A. D. Marwick and F. K. LeGoues, *Phys. Rev. B: Condens. Matter*, 1991, **44**, 1861–1874.
20 D. Szczuko, D. Werner, S. Oswald, G. Behr and K. Wetzig, *Appl. Surf. Sci.*, 2001, **179**, 301–306.

 This journal is © The Royal Society of Chemistry 2012